Catalysis Today 157 (2010) 125–130

Contents lists available at ScienceDirect

Catalysis Today

journal homepage: www.elsevier.com/locate/cattod

Total oxidation of benzene and chlorobenzene with MoO_3- and WO_3-promoted V_2O_5/TiO_2 catalysts prepared by a nonhydrolytic sol–gel route

Damien P. Debecker[a], Romain Delaigle[a], Karim Bouchmella[b], Pierre Eloy[a], Eric M. Gaigneaux[a], P. Hubert Mutin[b,*]

[a] Université catholique de Louvain, Institute of Condensed Matter and Nanosciences - IMCN, Division « MOlecules, Solids and reactiviTy – MOST », Croix du Sud 2/17, B-1348 Louvain-la-Neuve, Belgium[#]
[b] Institut Charles Gerhardt, UMR 5253, CNRS-UM2-ENSCM-UM1, Université Montpellier 2, cc 1701, Montpellier 34095, France

ARTICLE INFO

Article history:
Available online 11 March 2010

Keywords:
Alkoxide
PCDD
SCR
XPS
End-of-pipe treatment
Rutile
Non-hydrolytic sol-gel

ABSTRACT

Vanadia–titania oxidation catalysts are highly regarded for the abatement of persistent air pollutants including aromatics, chlorinated aromatics, furans and dioxins in gas effluents. Molybdenum and tungsten oxides are recognized as efficient promoters enhancing the efficiency of vanadia-based catalysts. Classical approaches for the preparation of promoted catalysts involve multi-step processes. Here, binary and ternary mixed oxide xerogels are formed in one step by nonhydrolytic condensation reactions of chloride precursors in non-aqueous medium. Calcination was applied to provoke the migration of active and promoting oxides toward the surface, leading to well-spread vanadium, molybdenum and tungsten oxide species on the surface of anatase particles. The resulting catalysts are mesoporous and their composition is precisely controlled, confirming the versatility and reliability of the preparation route. The samples perform well in the deep oxidation of benzene and chlorobenzene, chosen as model volatile organic compounds (VOC). The performances of ternary catalysts systematically exceed those of binary V_2O_5-TiO_2, highlighting the promoting effect of WO_3 and MoO_3.

1. Introduction

V_2O_5-TiO_2 catalysts are well-known efficient catalysts for the total oxidation of various air pollutants including aromatics, chlorinated aromatics, furans and dioxins [1]. They are also well-known for their good activity in the selective catalytic reduction (SCR) of NO_x [2]. The addition of MoO_3 or WO_3 in the formulation is reported to enhance the catalytic activity both in the reduction of NO_x [3] and in the abatement of VOC like chlorobenzene [4], benzene [5] and dibenzofuran [6]. V_2O_5-MoO_3/TiO_2 or V_2O_5-WO_3/TiO_2 catalytic formulations thus constitute an important field of research and development dedicated to the improvement of air pollution control technologies [7–8].

Classical methods for the preparation of V_2O_5-MoO_3/TiO_2 or V_2O_5-WO_3/TiO_2 catalysts involve one-step or multi-step wet impregnation on titania supports. These approaches present several downsides including inhomogeneity of the deposit(s) [9] and multi-step processes. As far as the preparation of binary V_2O_5/TiO_2 catalysts is concerned, alternative methods have already been proposed, including flame spray pyrolysis [9–10], grafting [11], hydrolytic [12–16] and nonhydrolytic sol–gel processes [17–18]. The latter methodology appears very promising as it allows producing catalysts in one step with an excellent control on the composition and on the textural properties. V_2O_5/TiO_2 catalysts prepared by this method exhibited very good activity in the total oxidation of benzene [18] and in the SCR of NO by ammonia [17]. To the best of our knowledge, no attempt was reported to produce catalysts from ternary oxide xerogels based on Ti, V and Mo or on Ti, V and W by nonhydrolytic sol–gel. Nonhydrolytic sol–gel chemistry has however proven quite successful for the tailored preparation of mixed oxides [19]. This method was already used to prepare ternary oxide catalysts including Si-V-Nb [20–22] Co-Al-Si [23], and very recently, efficient olefin metathesis catalysts based on ternary Si-Al-Mo oxides [24].

In this paper, a nonhydrolytic sol–gel route involving the reaction of metal chlorides with diisopropyl ether is used to prepare ternary mixed oxide gels based on Ti, V and Mo or based on Ti, V and W (Scheme 1). After vacuum drying, the resulting xerogels are calcined to give the catalysts. The calcination step aims to remove organic and chloride groups and to provoke the migration of V (and Mo or W) oxide species toward the catalyst surface, taking advantage of the low Tammann temperature of these oxides [13,18,24]. It should be noted that the terms "binary" and "ternary" catalysts only refer to the number of oxides involved in the formulations and not

* Corresponding author. Tel.: +33 4 6714 4943; fax: +33 4 6714 3852.
E-mail address: hubert.mutin@univ-montp2.fr (P.H. Mutin).
[#] IMCN and MOST are new research entities involving the group formerly known as Unité de catalyse et chimie des matériaux divisés.

0920-5861/$ – see front matter © 2010 Elsevier B.V. All rights reserved.
doi:10.1016/j.cattod.2010.02.010

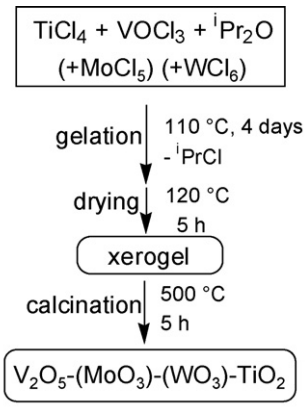

Scheme 1. Schematic representation of the nonhydrolytic sol–gel preparation method.

to the fact that the materials are homogeneous bulk mixed oxides. While the xerogels are indeed supposed to be homogeneous, the expected effect of calcination is to reach a situation where the active and promoting oxides are preferentially located at the surface of the catalyst. This strategy was monitored by XPS and XRD. The structure and texture of the catalysts are studied using N_2-physisorption, XRD, SEM and TEM and are correlated to their performances in the total oxidation of benzene and chlorobenzene.

2. Experimental

2.1. Preparation of the catalysts

Manipulations were carried out under argon atmosphere, CH_2Cl_2 (VWR, 100%) and diisopropyl ether ($^iPr_2O$, Acros Organics, 99%) were dried before use. The mixed oxides were prepared in 2 g quantities. Vanadyl chloride ($VOCl_3$, Aldrich, 99%), titanium chloride ($TiCl_4$, Acros Organics, 99.9%), molybdenum chloride ($MoCl_5$, Alfa Aesar, 99.6%) and/or tungsten chloride (WCl_6, Alfa Aesar, 99%) were first introduced in a glass tube. The stoichiometric amount of diisopropyl ether ($^iPr_2O$, Acros Organics, 99%) was added and finally 20 ml of CH_2Cl_2 (VWR) for 2 g of mixed oxide. The sealed tube was heated at 110 °C in an oven for 4 days under autogeneous pressure. The resulting gel was dried under vacuum at 120 °C for 5 h and then calcined under dry air at 500 °C for 5 h (heating rate 10 °C min^{-1}). Catalysts are denoted TiV*x*, TiV*x*Mo or TiV*x*W where *x* represents the nominal weight loading of V_2O_5, in %. Nominal loadings of 3, 5 and 10 wt% were explored. Doping with Mo or W trioxides was always done with 5% nominal weight loading of the oxide.

2.2. Catalytic tests

Catalytic tests were performed in an inconel fixed-bed microreactor of 1 cm internal diameter (PID ENG&Tech, Spain, Madrid) operating at atmospheric pressure. The catalytic bed was composed of 200 mg of catalyst powder selected within the 200–315 μm granulometric fraction and diluted in 800 mg of inactive glass spheres with diameters in the range 315–500 μm. The gas stream contained 100 ppm of benzene in He (Praxair), 20% of O_2 (Praxair; 99.995%) and He (Praxair; 99.996%) as diluting gas to obtain 200 ml min^{-1} (VVH = 37 000 h^{-1}). The conversion was measured at 300 °C after a stabilization time of about 100 min. Conversion is defined as the ratio transformed reactant/reactant in the inlet (in %). Analysis of reactants and products was continuously performed by on-line gas chromatography (GC). A CP-3800 gas chromatography apparatus from Varian equipped with four columns (one Hayesep G, one Hayesep T, one Molsieve and one CP-Sil 8CB) and three detectors (one TCD and two FID) was used with He as carrier gas in order to quantify benzene, O_2, CO, CO_2 and to detect other hydrocarbons. The analysis parameters allowed one analysis each 15 min accurate within about 1% (relative) for the conversion of benzene or chlorobenzene.

2.3. Catalysts characterization

X-ray diffraction (XRD) measurements were performed on the fresh catalysts with a Siemens D5000 difractometer using the Kα radiation of Cu (λ = 1.5418 Å).

The weight percentages of V, Mo, W and Ti were measured by Inductively Coupled Plasma-Atomic Emission Spectroscopy (ICP-AES) on an Iris Advantage apparatus from Jarrell Ash Corporation.

N_2-physisorption experiments were performed at −196 °C on a Micromeritics Tristar. The samples were outgassed for 6 h at 200 °C under vacuum (2 Pa). The specific surface area was determined from the adsorption isotherm in the 0.05–0.30 P/P_0 range using the BET method. The pore size distribution, mean pore diameter and pore volume were derived from the desorption branch using the BJH method.

X-ray photoelectron spectroscopy (XPS) analyses were performed on a SSX 100/206 photoelectron spectrometer from Surface Science Instruments (USA) equipped with a monochromatised microfocus Al X-ray source (powered at 20 mA and 10 kV). The samples powders pressed in small stainless steel troughs of 4 mm diameter were placed on a ceramic carousel. The pressure in the analysis chamber was around 10^{-6} Pa. The angle between the surface normal and the axis of the analyzer lens was 55°. The analyzed area was approximately 1.4 mm^2 and the pass energy was set at 150 eV. In these conditions, the resolution determined by the full width at half maximum (FWHM) of the Au $4f_{7/2}$ peak was around 1.6 eV. A flood gun set at 10 eV and a Ni grid placed 3 mm above the sample surface were used for charge stabilization. Following sequence of spectra was recorded: survey spectrum, C 1s, O 1s together with V 2p, Ti 2p, Cl 2p, Mo 3d or W 4d and C 1s again to check the stability of charge compensation in function of time and the absence of degradation of the sample during the analyses. Because of overlapping of Ti 3p and W 4f (usually chosen for tungsten analysis), W 4d region was preferred. The binding energies were calculated with respect to the C-(C,H) component of the C 1s peak fixed at 284.8 eV. Data treatment was performed with the CasaXPS program (Casa Software Ltd., UK). Molar fractions were calculated using peak areas normalized on the basis of acquisition parameters and sensitivity factors provided by the manufacturer.

Scanning Electron Micrographs were obtained with a HITACHI-S4800 electron microscope.

Transmission Electron Microscopy (TEM) was conducted on a LEO922 electron microscope operating at 200 keV. The powdered samples, dispersed in 2-butanol, were deposited on copper grids coated with a porous carbon film and the solvent was then evaporated.

3. Results and discussion

3.1. Texture, composition and structure

The catalysts had a specific surface area (SSA) between 53 and 109 m^2g^{-1} (Table 1). N_2 adsorption–desorption isotherms were of type IV, according to the BDDT classification, confirming that all the samples were mesoporous. The pore size distribution was always relatively narrow (not shown) and centered around 10 nm, as previously reported for binary V_2O_5/TiO_2 catalysts [18].

It was already reported, that the nonhydrolytic sol–gel preparation method offered an excellent control on the composition of Ti-V or Si-Al-Mo mixed oxides [18,24]. This was verified for the TiV3,

Table 1
Textural properties obtained by N_2-physisorption.

Generic name	SSA ($m^2\ g^{-1}$)	Pore diameter (nm)	Pore volume ($cm^3\ g^{-1}$)
TiV3	88	10.9	0.32
TiV3Mo	86	9.9	0.30
TiV3W	109	8.9	0.34
TiV5	64	10.7	0.18
TiV5Mo	90	8.5	0.19
TiV5W	58	8.9	0.13
TiV10	71	11.5	0.22
TiV10Mo	53	11.2	0.15
TiV10W	93	11.3	0.26

TiV3Mo and TiV3W formulations (Table 2) using ICP-AES elementary analysis. The nonhydrolytic route used in this study to prepare ternary mixed oxide catalysts obviously allows a very good control on the composition as attested by the excellent agreement between expected and experimental compositions.

Fig. 1 shows SEM micrographs of the SG-TiV3Mo sample taken as a representative example of all other samples (except TiV10Mo; see below). The catalysts can be described as aggregates of spherical micrograins of about 2–5 μm sometimes partially fused together (Fig. 1a). The surface of these micrograins appears to be smooth on Fig. 1b but the textural properties described above indicate that they are porous. Indeed, at higher magnification they appear clearly formed by an agglomeration of small elementary nanoparticles (Fig. 1c) in the 10–25 nm range (Fig. 1d). The mesoporous texture described above can be correlated to the morphology of the catalysts as observed in SEM: the porosity results from the interspaces between the well-calibrated nanoparticles in the micrograins, leading to a quite narrow pore size distribution.

The TiV10Mo sample differed from the other catalysts. The surface of the spherical aggregates was less smooth and acicular structures were observed (Fig. 2a). Transmission electron microscopy images also revealed the presence of additional rod-like structures (Fig. 2b), suggesting the growth of a crystalline phase.

3.2. Crystallinity (XRD)

The crystallinity of the catalysts was investigated by XRD (Fig. 3). Most samples only exhibited diffraction peaks related to

Table 2
Composition of the samples (ICP-AES).

Generic name	Expected composition[a] Ti: V: Mo: W (in %)	Ti (%)	V (%)	Mo (%)	W (%)
TiV3	58.4: 1.5: 0: 0	58.4	1.5	0	0
TiV3Mo	55.3: 1.9: 3.5: 0	55.0	1.9	3.3	0
TiV3W	54.8: 1.8: 0: 3.6	55.4	1.8	0	3.5

[a] Calculated from the amount of reactant involved in each preparation.

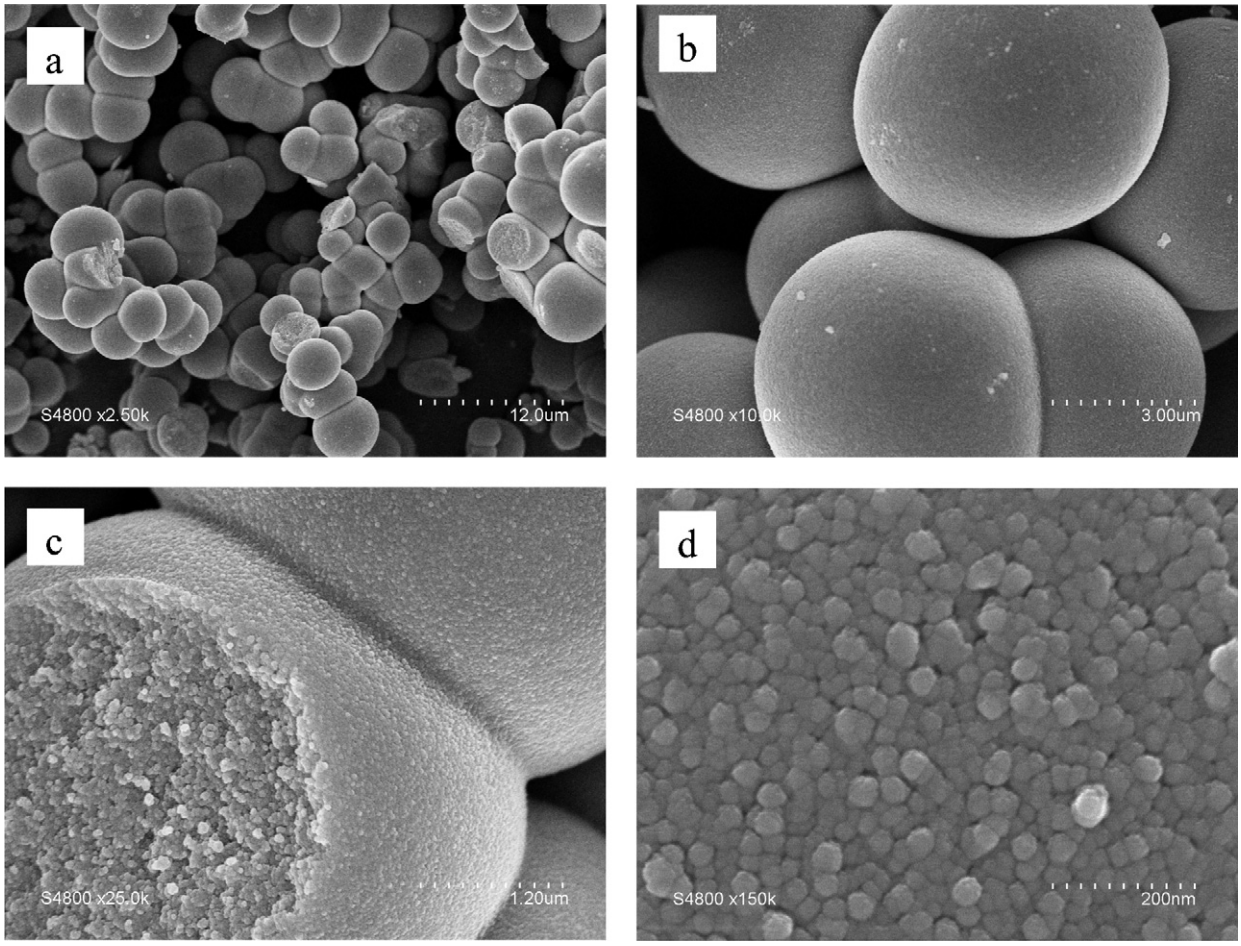

Fig. 1. SEM micrographs on the TiV3Mo at different magnitudes. Very similar images were obtained for all other samples (except TiV10Mo). Scale bars represent 12 μm, 3 μm, 1.2 μm and 200 nm respectively for (a), (b), (c) and (d).

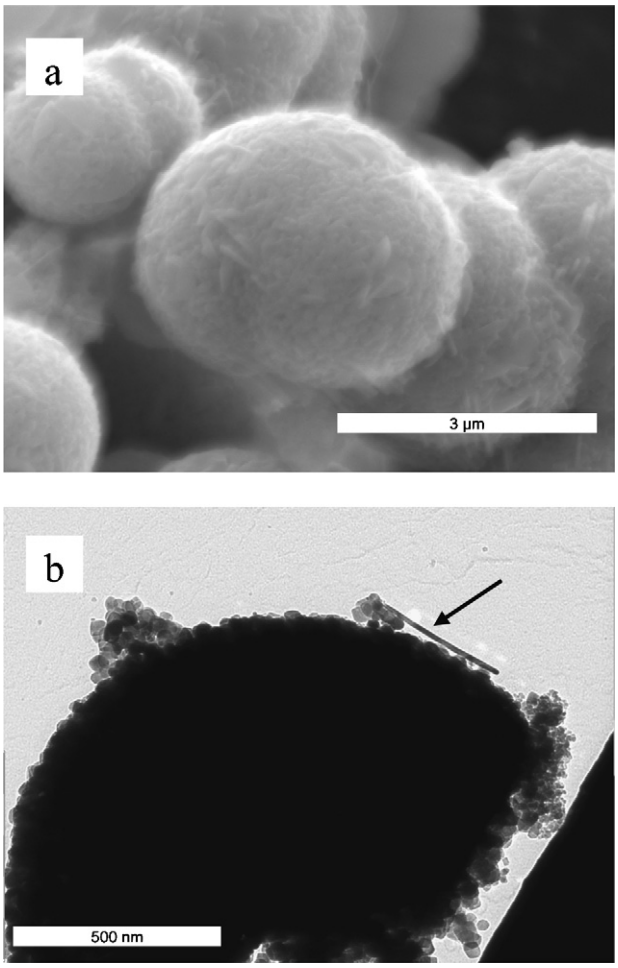

Fig. 2. (a) SEM micrograph of the TiV10Mo sample (scale bar = 3 μm). (b) TEM micrograph of one micronic particle of TiV10Mo. The arrow indicates the rod-like structures observed on TiV10Mo (but never on the other samples).

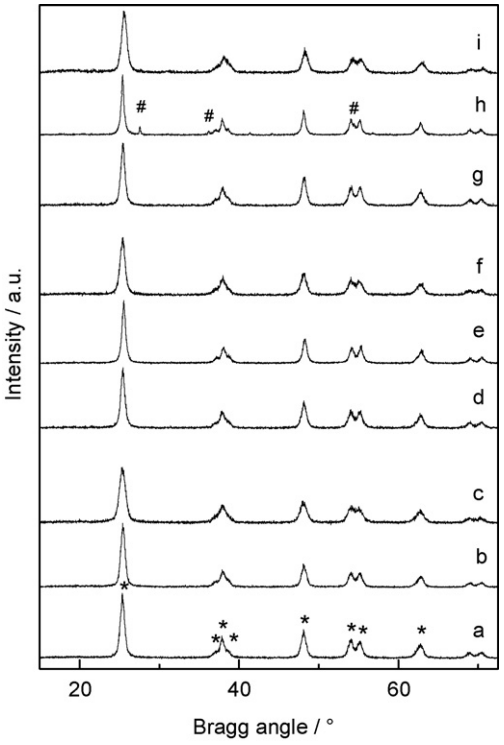

Fig. 3. X-ray diffraction patterns. (a) TiV3, (b) TiV3Mo, (c) TiV3W, (d) TiV5, (e) TiV5Mo, (f) TiV5W, (g) TiV10, (h) TiV10Mo and (i) TiV10W. "*" and "#" marks indicate the diffraction lines attributed to anatase and rutile respectively.

anatase (main peaks at 25.3°, 37.0°, 37.8°, 38.6°, 48.1°, 53.9°, 55.1°, 62.6° according to JCPDS 21-1272). Studies on V_2O_5/TiO_2 catalysts prepared by wet impregnation [25] concluded that anatase was particularly interesting, as compared to other crystallographic forms of TiO_2 because the wetting of anatase by V_2O_5 was optimal [26]. So the fact that the one-step preparation of such binary and ternary mixed oxides by nonhydrolytic sol–gel, followed by calcination at 500 °C mainly leads to anatase is encouraging. The only exception concerned the catalyst loaded with 10 wt% V_2O_5 and with 5 wt% MoO_3 (TiV10Mo) in which rutile was also detected. It seems that the anatase-to-rutile transition was favored in this sample by the combined presence of a high amount of V_2O_5 and of MoO_3. This anatase-to-rutile transition usually occurs at higher temperature than the calcination temperature employed here (500 °C) but it is well-documented that the presence of other oxides in the material can induce a lowering of the phase transition temperature [14]. The formation of rutile apparently correlates with the presence of the acicular structures observed on this sample in SEM and of the rod-like structures observed in TEM (Fig. 2).

No crystalline vanadium oxide was detected even for the highest loading (10 wt% V_2O_5).

Similarly, no crystalline molybdenum oxide was detected in the Mo-promoted catalysts. In addition, the doping with Mo did not provoke any change in the crystallinity in the SG-TiV3Mo and in the TiV5Mo catalysts, as compared to the corresponding unpromoted samples (Fig. 3). In the case of TiV10Mo, the appearance of a rutile phase was concomitant with a growth of the anatase crystallites, as shown by the sharper anatase peaks.

No crystalline W oxide was detected in the W-promoted samples prepared by nonhydrolytic sol–gel. This is remarkable because diffraction peaks corresponding to WO_3 crystallites (at 24° and 34°, following JCPDS 32-1395) are usually observed when V_2O_5-WO_3/TiO_2 formulations with such W loadings are prepared by classical wet impregnation [4–5]. It is noteworthy that the anatase peaks are systematically broader in W-promoted samples as compared to samples with only V or with V and Mo. The presence

Table 3
Surface composition determined by XPS.

		V (%)	Mo (%)	W (%)	C (%)	Cl (%)	Ti (%)	V/Ti	Mo/Ti	W/Ti
TiV3[a]	Fresh	0.4	–	–	27.4	2.7	17.1	0.023	–	–
	Calcined	1.2	–	–	16.8	0.3	20.9	0.059	–	–
TiV3Mo	Fresh	0.5	0.6	–	30.5	2.4	16.1	0.030	0.039	–
	Calcined	1.2	2.0	–	15.4	0.3	20.0	0.059	0.099	–
TiV3W	Fresh	0.5	–	0.2	38.2	2.5	14.4	0.036	–	0.013
	Calcined	1.0	–	0.4	18.1	0.4	20.4	0.050	–	0.021

[a] Data reproduced from Ref. [17].

of W seems to hinder the growth of anatase crystallites in these samples.

3.3. Surface analysis (XPS)

The TiV3 catalyst and the corresponding promoted formulations were analyzed by XPS before and after calcination (Table 3). Important chlorine (~2.5 at.%) and carbon (27–38 at.%) contents were detected at the surface of the xerogels (before calcination). This has to be related to the nature of the precursors used and of the alkyl chlorides released during the formation of the gels. Calcination resulted in the removal of most of the Cl as indicated by the signal reduced to about 10–15% of the initial value found for the fresh xerogels. The C surface content of the xerogels exceeded the level of natural C contamination typically found on such catalysts (15–20 at.%) [4,27–29]. Calcination resulted in the removal of these organic groups as attested by the drop in the carbon atomic surface concentration. The remaining C can then be attributed to the usual organic contamination that is always present at the surface of such solids stored under ambient air.

The V/Ti, Mo/Ti and W/Ti atomic ratios determined by XPS for the xerogels (Table 3) give an indication about their homogeneity. The experimental V/Ti values are very close to the expected V/Ti ratios calculated from the nominal composition of the samples (0.024, 0.032 and 0.031 respectively for TiV3, TiVMo and TiVW). Similarly, the Mo/Ti and W/Ti ratio determined at the surface of the xerogels are in the same range as the expected ratio (0.032 and 0.017 respectively for TiV3Mo and TiV3W). This shows that the xerogels are initially quite homogeneous, each metal being statistically dispersed in the matrix of the materials.

After calcination, the atomic surface concentrations of V, Mo, W and Ti increased (Table 3). This could be attributed to the cleaning of the inorganic surface through the removal of organic and chlorinated species. However, the M/Ti ratios (M = V, Mo, W) also increased significantly, indicating an enrichment of the surface in V (and in Mo or W). This migration of active metal oxide species toward the surface of TiO_2 as a result of thermal treatment has already been evidenced in the case of V-Ti systems [18,30] but also in the case of Mo atoms migrating in a mixed Mo-Si-Al oxide obtained by nonhydrolytic sol–gel [24]. This migration is correlated to the fact that the temperature at which the calcination has been performed (500 °C) is well above the Tammann temperature of V (209 °C) and Mo (261 °C) oxides and approaches the Tammann temperature of W oxide (600 °C). Above the Tammann temperature of a solid, the displacements of atoms in the solid are possible and the material is potentially subjected to phenomena like sintering, migration, diffusion, etc. The limited solubility of V, Mo and W oxides in anatase is the driving force for these movements. This phenomenon is less marked for W than for Mo and V, as W/Ti increases less after calcination than V/Ti and Mo/Ti, consistent with the higher Tammann temperature of W oxide.

Thus, as a result of calcination, the distribution of the V, Mo and/or W atoms into the material is affected. A high proportion of the V (and Mo or W) content is located at their surface. However, V, Mo and W surface concentrations were systematically lower for the catalysts prepared by nonhydrolytic sol–gel in this study than for catalysts prepared by wet impregnation with similar compositions [4]. It can be evaluated that the atomic surface concentrations in the calcined xerogels are about 20%, 40% and 70% lower respectively for V, Mo and W than the corresponding surface concentrations found in catalysts where both the active and promoting oxides are directly deposited onto the support (like in WI). The migration of V, Mo and W was thus incomplete. As noted above, the anatase crystallites were smaller in the case of W-promoted catalysts (Fig. 3), suggesting that the crystallization of anatase is retarded because part of the W species remains in the bulk of the material.

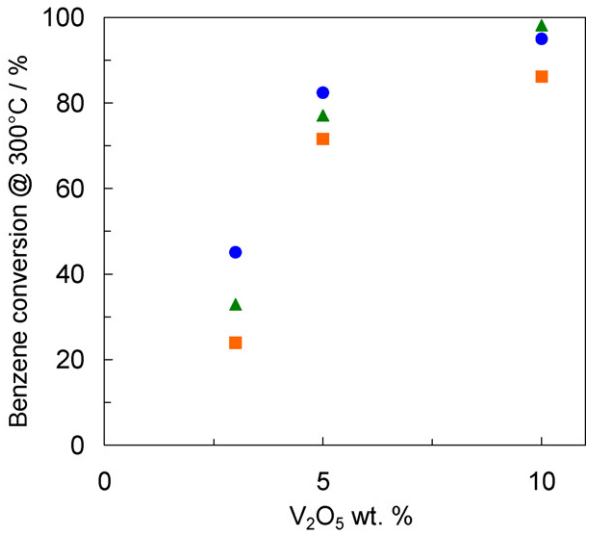

Fig. 4. Activity measured in the total oxidation of benzene at 300 °C with (■) TiVx, (▲) TiVxW and (●) TiVxMo. No deactivation was observed during the 150 min test.

3.4. Activity measurements

3.4.1. Benzene total oxidation

The impact of the doping with Mo and W oxides has been studied for the three V_2O_5 loadings envisaged here. Fig. 4 gives the conversion obtained with promoted and unpromoted catalysts at 300 °C. Note that the selectivity for CO_2 was always very high, with only traces of CO detected. For each V_2O_5 loading, a significant increase in activity was observed when Mo or W was added. This result shows that the promoting effect of Mo and W oxides did occur in our catalysts and that the preparation of such catalytic formulations can be done through this one-step nonhydrolytic sol–gel method. Furthermore, the conversion measured here compared well with the results obtained with similar formulations prepared by classical routes and tested in the same set-up (results recently reviewed [1]). Two additional observations can be made. On the one hand, at low and medium V_2O_5 loading, MoO_3 appeared as a better promoter than W since TiV3Mo and TiV5Mo catalysts perform better than TiV3W and TiV5W. This is consistent with the incomplete migration of W species leading to low W surface concentration. On the other hand, at high V_2O_5 loading, the TiV10Mo catalyst was less active than the TiV10W one. This can tentatively be attributed to the partial anatase-to-rutile phase transition and the growth of rutile crystallites observed in the TiV10Mo sample (Fig. 3).

3.4.2. Chlorobenzene total oxidation

Chlorobenzene is often taken as a model for dioxins. However, studies have shown that the behavior of polychlorinated dibenzo-p-dioxins (PCDD) and polychlorinated dibenzofurans (PCDF) could be better modeled with compounds like furan or 2,5-dimethylfuran [4,28]. The choice of the model compound can have a strong influence on the conclusions of studies aiming at the development of improved catalytic formulations [31]. For example Mo and W promoting of V_2O_5/TiO_2 catalysts was reported as deleterious for the abatement of furan and 2,4-dimethylfuran but beneficial for the abatement of benzene and chlorobenzene [4,28]. The relevance of this doping strategy for the precise purpose of dioxin abatement is thus still under debate.

Nevertheless it is crucial to assess the resistance of VOC total oxidation catalysts toward chlorine poisoning. Indeed, deactivation provoked by chlorine would be problematic in the case of industrial plants where chlorinated pollutants – including dioxins – are to be abated. The performances of the three best catalysts

Table 4
Activity of the catalysts in the total oxidation of chlorobenzene at 300 °C. No deactivation was observed during the 150 min tests.

	Conversion (%)
TiV10	75
TiV10Mo	93
TiV10W	93

presented in this study were thus also measured in the total oxidation of chlorobenzene and the promoting effect of Mo and W oxides was checked. Table 4 shows that the TiV10 sample converted 75% of chlorobenzene at 300 °C, which is somewhat lower than the conversion measured in the total oxidation of benzene. However, both promoted catalysts performed significantly better, reaching 93% conversion at 300 °C. This result confirms the promoting effect of Mo and W oxides in the total oxidation of a chlorinated VOC by ternary catalysts prepared in one step by nonhydrolytic sol–gel.

Note that long term experiments and catalytic tests on complex effluents flows should be carried out in order to validate these new catalytic materials for plant applications. As expected [27], the presence of chlorine did not affect the stability of the catalyst and no deactivation was observed during the 150 min catalytic tests at 300 °C. In addition, the amount of Cl detected by XPS at the surface of the catalyst remained very low (ca. 0.4 at.%), showing that no Cl build up occurred during the reaction.

3.5. Promoting effect of Mo and W oxides

The promoting of Mo and W oxides on the total oxidation activity of V_2O_5/TiO_2 catalysts has been mainly demonstrated by studying catalysts prepared by conventional impregnation methods [4,5,28,32]. It is worth mentioning that Mo and W oxides when supported alone on TiO_2 are poorly active in the total oxidation of VOC [4]. The synergy between V and Mo or W oxides was attributed to the additional Brönsted acidity brought by the promoter. Such acidic sites are thought to favor the adsorption of the pollutant. This strategy is shown here to be also relevant in systems prepared by nonhydrolytic sol–gel, since doping systematically resulted in a significant increase in activity. Mo and W oxides thus bring additional performances not only when deposited onto the TiO_2 support through an impregnation method but also when arising from the bulk of a homogeneous xerogel.

4. Conclusions

This work has investigated the possibility to prepare through a simple nonhydrolytic sol–gel route TiO_2/V_2O_5 catalysts promoted by WO_3 or MoO_3, dedicated to the total oxidation of atmospheric pollutants. It is demonstrated that the nonhydrolytic sol–gel route used here offers simultaneous control on the composition, the texture (mesoporous samples with high surface area) and the structure of the catalysts based on anatase particles with high surface concentration of both the active and promoting species. The other advantages of this route are its simplicity (one-step, no templating agent or elaborate drying procedure), its versatility (a large variety of mixed oxides can be obtained), and the commercial availability and low cost of the chlorides precursors. Calcination of the homogeneous xerogels leads to the migration of V, Mo and W species toward the surface of the anatase particles. Decreasing efficiency of this phenomenon in the order V > Mo > W correlates with the increasing Tammann temperature of V_2O_5, MoO_3 and WO_3.

Benzene and chlorobenzene were used as model VOCs to assess the relevance of the nonhydrolytic sol–gel preparation method. The catalysts are efficient in the total oxidation of benzene and chlorobenzene, comparing very well with other classically prepared samples. Moreover, the well-known promoting effect of MoO_3 and WO_3 on the active V_2O_5 is also demonstrated in the case of these nonhydrolytic sol–gel prepared catalysts.

Acknowledgments

This work was initiated and supported by the «FAME» Network of Excellence of the EU 6th FP. The authors gratefully acknowledge the UCLouvain, the Fonds National de Recherche Scientifique (FNRS) in Belgium, the Ministère de l'Enseignement Supérieur et de la Recherche and the Centre National de la Recherche Scientifique (CNRS) in France for financial support. D.P. Debecker acknowledges the FNRS for his Research Fellow position. R. Delaigle thanks the FRIA for his PhD Student position. The involvements of Unité de catalyse et chimie des matériaux divisés in the «Inanomat» IUAP network sustained by the «Service public fédéral de programmation politique scientifique» (Belgium) and in the Cost Action D41 sustained by the European Science Foundation are also acknowledged. The authors thank the Belgian Funds for Collective Fundamental Research (FRFC) and the FNRS supporting the acquisition of the TEM and XPS.

References

[1] R. Delaigle, D.P. Debecker, F. Bertinchamps, E.M. Gaigneaux, Top. Catal. 52 (2009) 501–516.
[2] A. Kruse, S. Kristensen, A. Riisager, S. Rasmussen, R. Fehrmann, J. Mater. Sci. 44 (2009) 323–327.
[3] B.W. Lee, H. Cho, D.W. Shin, J. Ceram. Process. Res. 8 (2007) 203–207.
[4] D.P. Debecker, F. Bertinchamps, N. Blangenois, P. Eloy, E.M. Gaigneaux, Appl. Catal. B 74 (2007) 223–232.
[5] F. Bertinchamps, C. Gregoire, E.M. Gaigneaux, Appl. Catal. B 66 (2006) 10–22.
[6] M.A. Larrubia, G. Busca, Appl. Catal. B 39 (2002) 343–352.
[7] L. Lazar, H. Koser, I. Balasanian, F. Bandrabur, Environ. Eng. Manage. J. 6 (2007) 13–20.
[8] C.C. Yang, S.H. Chang, B.Z. Hong, K.H. Chi, M.B. Chang, Chemosphere 73 (2008) 890–895.
[9] B. Schimmoeller, R. Delaigle, D.P. Debecker, E.M. Gaigneaux, Flame-made vs. wet-impregnated vanadia/titania in the total oxidation of chlorobenzene: Possible role of VO_x species, Catal. Today (2010), doi:10.1016/j.cattod.2010.01.029.
[10] B. Schimmoeller, H. Schulz, A. Ritter, A. Reitzmann, B. Kraushaar-Czametzki, A. Baiker, S.E. Pratsinis, J. Catal. 256 (2008) 74–83.
[11] F. Chiker, J.P. Nogier, J.L. Bonardet, Catal. Today 78 (2003) 139–147.
[12] X. Zhang, X.G. Li, J.S. Wu, R.C. Yang, Z.H. Zhang, Catal. Lett. 130 (2009) 235–238.
[13] J.P. Balikdjian, A. Davidson, S. Launay, H. Eckert, M. Che, J. Phys. Chem. B 104 (2000) 8931–8939.
[14] S. Djerad, L. Tifouti, M. Crocoll, W. Weisweiler, J. Mol. Catal. A: Chem. 208 (2004) 257–265.
[15] I.M. Pearson, H. Ryu, W.C. Wong, K. Nobe, Ind. Eng. Chem. Prod. Res. Dev. 22 (1983) 381–382.
[16] C.B. Rodella, R.W.A. Franco, C.J. Magon, J.P. Donoso, L.A.O. Nunes, M.J. Saeki, M.A. Aegerter, A.O. Florentino, J. Sol–gel Sci. Technol. 25 (2002) 75–82.
[17] P.H. Mutin, A.F. Popa, A. Vioux, G. Delahay, B. Coq, Appl. Catal. B 69 (2006) 50–58.
[18] D.P. Debecker, K. Bouchmella, R. Delaigle, P. Eloy, C. Poleunis, P. Bertrand, E.M. Gaigneaux, P.H. Mutin, Appl. Catal. B 94 (2010) 38–45.
[19] P.H. Mutin, A. Vioux, Chem. Mater. 21 (2009) 582–596.
[20] F. Barbieri, D. Cauzzi, F. De Smet, M. Devillers, P. Moggi, G. Predieri, P. Ruiz, Catal. Today 61 (2000) 353–360.
[21] P. Moggi, M. Devillers, P. Ruiz, G. Predieri, D. Cauzzi, S. Morselli, O. Ligabue, Catal. Today 81 (2003) 77–85.
[22] P. Moggi, G. Predieri, D. Cauzzi, M. Devillers, P. Ruiz, S. Morselli, O. Ligabue, Stud. Surf. Sci. Catal. 143 (2002) 149–157.
[23] B.L. Caetano, L.A. Rocha, E. Molina, Z.N. Rocha, G. Ricci, P.S. Calefi, O.J. de Lima, C. Mello, E.J. Nassar, K.J. Ciuffi, Appl. Catal. A 311 (2006) 122–134.
[24] D.P. Debecker, K. Bouchmella, C. Poleunis, P. Eloy, P. Bertrand, E.M. Gaigneaux, P.H. Mutin, Chem. Mater. 21 (2009) 2817–2824.
[25] F. Bertinchamps, C. Gregoire, E.M. Gaigneaux, Appl. Catal. B 66 (2006) 1–9.
[26] M. Gasior, J. Haber, T. Machej, Appl. Catal. 33 (1987) 1–14.
[27] F. Bertinchamps, C. Poleunis, C. Gregoire, P. Eloy, P. Bertrand, E.M. Gaigneaux, Surf. Interface Anal. 40 (2008) 231–236.
[28] D.P. Debecker, R. Delaigle, P. Eloy, E.M. Gaigneaux, J. Mol. Catal. A: Chem. 289 (2008) 38–43.
[29] D.P. Debecker, C. Faure, M.E. Meyre, A. Derre, E.M. Gaigneaux, Small 4 (2008) 1806–1812.
[30] U. Scharf, M. Schneider, A. Baiker, A. Wokaun, J. Catal. 149 (1994) 344–355.
[31] J.E. Lee, J. Jurng, Catal. Lett. 120 (2008) 294–298.
[32] E. Finocchio, M. Baldi, G. Busca, C. Pistarino, G. Romezzano, F. Bregani, G.P. Toledo, Catal. Today 59 (2000) 261–268.